

# Micro transfection on a metallic stick: an innovative approach of reflection infrared spectroscopy for minimally invasive investigation of painting varnishes

Francesca Rosi<sup>1</sup> · Lea Legan<sup>2</sup> · Costanza Miliani<sup>1</sup> · Polonca Ropret<sup>2,3</sup>

Received: 25 October 2016 / Revised: 29 December 2016 / Accepted: 13 February 2017 / Published online: 6 March 2017  
© Springer-Verlag Berlin Heidelberg 2017

**Abstract** A new analytical approach, based on micro-transfection measurements from a diamond-coated metal sampling stick, is presented for the analysis of painting varnishes. Minimally invasive sampling is performed from the varnished surface using the stick, which is directly used as a transfection substrate for micro Fourier transform infrared (FTIR) measurements. With use of a series of varnished model paints, the micro-transfection method has been proved to be a valuable tool for the identification of surface components thanks to the selectivity of the sampling, the enhancement of the absorbance signal, and the easier spectral interpretation because the profiles are similar to transmission mode ones. Driven by these positive outcomes, the method was then tested as tool supporting noninvasive reflection FTIR spectroscopy during the assessment of varnish removal by solvent cleaning on paint models. Finally, the integrated analytical approach based on the two reflection methods was successfully applied for the monitoring of the cleaning of the sixteenth century painting *Presentation in the Temple* by Vittore Carpaccio.

**Keywords** Varnishes · Micro fourier transform infrared spectroscopy · Reflection spectroscopy · Artworks · Cleaning

✉ Francesca Rosi  
francesca.rosi@cnr.it

<sup>1</sup> Istituto di Scienze e Tecnologie Molecolari (CNR-ISTM), Via Elce di sotto 8, 06123 Perugia, Italy

<sup>2</sup> Institute for the Protection of the Cultural Heritage of Slovenia, Poljanska cesta 40, 1000 Ljubljana, Slovenia

<sup>3</sup> Museum Conservation Institute, Smithsonian Institution, 4210 Silver Hill Road, Suitland, MD 20746, USA

## Introduction

Cleaning of easel paintings often poses the challenge of selective removal of unoriginal varnish coatings applied in earlier restoration interventions. To reestablish the original appearance of the painting, it can be necessary to selectively remove the top coatings, usually darkened by oxidation processes and dirt deposition, while preserving the original layer of paint underneath. To perform a safe and effective cleaning treatment, the best practice would include firstly the molecular identification of the organic varnish/es to be removed so as to select the most appropriate solvent. Secondly, once the cleaning method has been optimized, an analytical tool able to follow carefully the removal of the unoriginal surface material is recommended. The challenge of an analytical method in monitoring painting cleaning is related to the very small thickness (typically a few microns) of varnish coatings. For that reason, a technique that requires no or very surface localized sampling needs to be applied for successful assessment of the cleaning procedure.

Fourier transform infrared (FTIR) spectroscopy is a well-established technique in the analysis of cultural heritage materials. The reliability of measurements with no or extremely small quantities of sample materials is very high. Transmission FTIR methods give well-defined spectra, but require sampling and sample manipulation, and hence are unsuitable for surface analysis. A valid alternative is offered by noninvasive FTIR reflection spectroscopy, which, although it has been already proved to be highly sensitive for the identification of surface compounds in monitoring cleaning treatments [1–4], poses some issues for spectral interpretation.

In this article we propose a new FTIR method for studying painting varnishes based on micro reflection. In more detail, a diamond-coated metallic stick, commercially available as an accessory for diffuse reflectance infrared Fourier transform (DRIFT) measurements [5], has been used here both as a

microsampling tool for painting surface materials and as a reflective substrate for micro-transflection measurements. By a gentle scratch of the varnish surface, the diamond-coated stick allows very localized and minimal sampling. The small amount of varnish spread on the metal stick is then analyzed in reflection mode through an FTIR microscope: the incident infrared beam may be transmitted through the sample, reflected by the metallic stick and transmitted again through the sample, approaching a transflection regime.

The transflection mode produces transmission-like spectra and provides high sensitivity for low infrared absorbing materials thanks to the double passage of the reflected light [6]. It is often exploited as low-cost and highly sensitive tool for biological and forensic applications [7–12], while the applications in the field of heritage science are a few and mainly related to the investigation of organic coating on metal artworks [13, 14]. During preliminary tests we recognized its potentiality also for studying painting materials [15].

In a typical transflection measurement, parameters such as the optical layout geometry (i.e., angle of incidence of infrared light), film thickness (uniformity), and substrate reflectivity are generally optimized to record reliable transflection profiles [13] and to limit the surface reflection and connected distortions.

The micro-reflection method presented here is based on recording the reflectance spectra from a paint material irregularly deposited (in term of thickness and geometry, which are also unknown and uncontrollable) on a reflective substrate (unpolished and relatively rough) with a fixed optical layout determined by the FTIR microscope (approximately 20°). We expect spectral distortions coming from a nonzero contribution of the surface and volume reflection [13]. Moreover, also in a pure transflection regime, spectral variations due to the reflection from a metallic-like surface generating electric-field standing waves (EFSWs) are expected [8, 12]. To evaluate these spectral distortions and their impact on the relative spectral interpretation for diagnostic purposes, the spectral profiles recorded from the sampling stick were compared with the corresponding transmission mode reference data. The comparison revealed good similarity, thus suggesting that the as-recorded spectra could be considered in a transflection regime.

Once the reliability of molecular identification by means of the (transflection mode) spectra had been demonstrated, micro transflection was evaluated as a method supporting noninvasive FTIR reflection for the monitoring of varnish removal by solvent cleaning.

## Materials and methods

### Laboratory models

Three different natural varnishes (namely, mastic, dammar, and egg white) were prepared following old recipes

[16, 17], and a synthetic varnish, Laropal A 81 was also selected as it is expected to be used in restoration procedures nowadays [18, 19]. The varnishes have the following compositions:

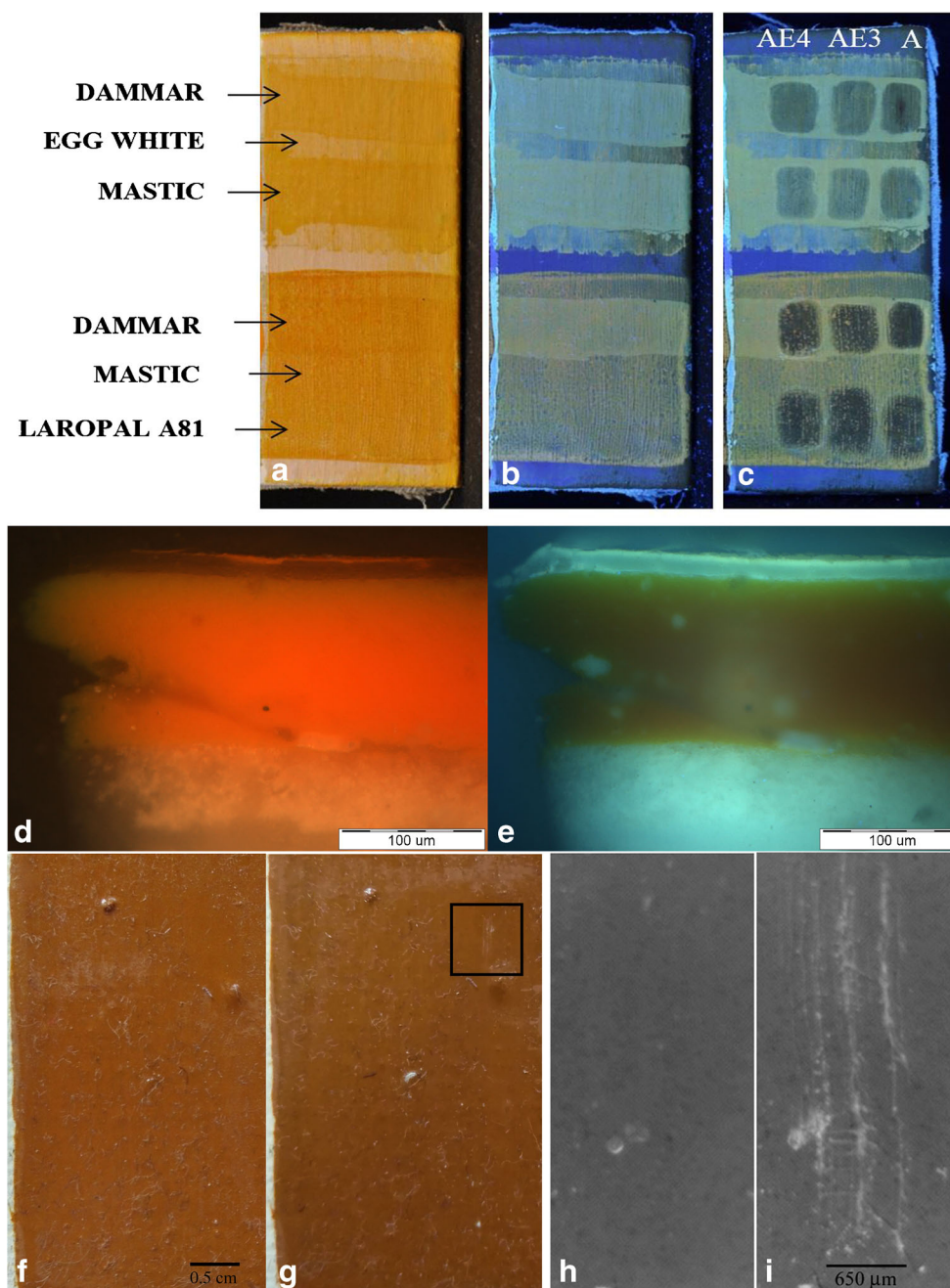
- Egg white: 27 g egg white, 54 g water, and 2 g white sugar
- Dammar: 30 g dammar (Kremer Pigmente, no. 60000), 120 g rectified turpentine (Kremer Pigmente, no. 70010), and 0.9 g Tinuvin 292 (3% by weight of dry dammar)
- Mastic: 20 g mastic (Kremer Pigmente, no. 60050), 60 g rectified turpentine (Kremer Pigmente, no. 70010), and 6 mL sun-bleached linseed oil (Lefrance & Bourgeois)
- Laropal A 81: Laropal A 81 urea–aldehyde resin (Kremer Pigmente, no. 67204), petroleum benzene (Merck), xylene (Merck), and 2% by weight of dry resin of Tinuvin 292 (Kremer Pigmente, no. 78152)

The model painting was prepared so as to imitate the typical structure of a canvas painting. Linen canvas was stretched across the wooden stretcher and impregnated with calcium carbonate ( $\text{CaCO}_3$ ) in animal glue, bound with size. Industrially prepared cadmium yellow deep oil paint (Van Dyck no. 15, Ferrario) containing CdS and magnesium hydroxide carbonate [ $4\text{MgCO}_3 \cdot \text{Mg}(\text{OH})_2 \cdot 4\text{H}_2\text{O}$ ] as a filler was applied on top of the ground layer. After drying, a layer of different varnishes was applied on top: egg white on the upper half of the model painting, and mastic varnish on its lower half (Fig. 1a, b). The model painting was then exposed to UV radiation from a metal halide lamp for 3 weeks. In the second week the relative humidity was increased to 60%. After this first cycle of aging, the second layer of varnishes was applied as follows: dammar and mastic varnishes were applied on top of the egg white layer, and dammar and Laropal A 81 were applied on the previously applied layer of mastic (Fig. 1a, b). Afterward, the model painting was exposed to the same UV conditions for another week. The visible and UV-induced fluorescence images of the cross section prepared from the model sample varnished with egg white and dammar are reported in Fig. 1d and e as examples of the layer stratigraphy.

### Cleaning tests

For the cleaning tests (Fig. 1c) acetone (supplied by Merck) and ethanol (supplied by Sigma-Aldrich) were used in different ratios: pure acetone, a mixture of acetone and ethanol in 3:7 volume ratio, and a mixture of acetone and ethanol in 4:6 volume ratio.

**Fig. 1** **a** Image of the model painting with the locations of the varnish layers marked. **b** UV-induced fluorescence image of the model painting before the cleaning treatments. **c** UV-induced fluorescence image of the model painting after cleaning with three different solvents (each vertical line of the cleaning tests corresponds to the cleaning agents labeled on top). **d** Visible and **e** UV-induced fluorescence images of the cross section of the model sample composed of a top varnished layer of mastic (5  $\mu\text{m}$  thick) over an egg white layer of varnish (20  $\mu\text{m}$  thick) applied on the CdS-based oil paint. Image of the model surface **f** before and **g** after the sampling with the stick; the *black square* in **g** indicates the sign left after the sampling; Microscopic visible images (in gray tone) of the model surface **h** before and **i** after the sampling with the stick. A acetone, AE3 3:7 v/v acetone and ethanol, AE4 4:6 v/v acetone and ethanol



### Sixteenth century painting

The Renaissance oil painting *Presentation in the Temple* (sixteenth century, Koper, Slovenia) by Vittore Carpaccio was the subject of a cleaning process monitored through the combined micro and noninvasive FTIR approach (Fig. 2a). The selected cleaning area is presented as a labeled square in Fig. 2a. This area was cleaned with different solvents and/or mixtures of solvents (Fig. 2b, c); namely, artificial saliva, white spirit, and mixtures of isooctane and ethanol in different volume ratios: 20:80 isooctane and ethanol, 40:60 isooctane and

ethanol, and 60:40 isooctane and ethanol (Fig. 2b, c). It was then analyzed with the two reflection FTIR methods.

### Micro-transfection FTIR spectroscopy

A diamond-coated metallic sampling stick (PerkinElmer; diamond-coated surface area 7 mm<sup>2</sup>), otherwise designed to be used with a DRIFT accessory, was used as both a sampling tool and an infrared-reflecting substrate for transfection exploiting the high hardness of the diamond coating and the high reflectivity of the metal underneath respectively. The



**Fig. 2** **a** Image of the Renaissance painting *Presentation in the Temple* with the cleaning test area marked (orange square). **b** Visible and **c** UV images corresponding to the different cleaning tests. *IE2* 20:80 isooctane and ethanol, *IE4* 40:60 isooctane and ethanol, *IE6* 60:40 isooctane and ethanol, *US* artificial saliva, *WS* white spirit



stick was gently rubbed over the (model) painting, leaving a trace that is barely visible to the naked eye as documented in Fig. 1f and g, where photographs of the surface before and after the sampling are reported. Magnification ( $\times 50$ ) of the same area (Fig. 1h, i before and after the sampling respectively) shows that only some thin and superficial scratches are produced. It is worth underlining that minimal sampling is also beneficial for the spectral quality since the lower the amount of sample deposited on the surface of the tip, the better the transfection effect.

The stick with the sample was affixed to a microscope slide with modeling mass and then examined under a Spotlight FTIR microscope with a  $\times 16$  Cassegrain objective.

Micro-FTIR reflection analyses were performed with a PerkinElmer Spectrum 100 FTIR spectrophotometer coupled to a Spotlight FTIR microscope equipped with a nitrogen-cooled mercury cadmium telluride detector. Data were acquired with aperture of  $50 \times 50 \mu\text{m}^2$ . Spectra were collected in reflection mode between  $7000$  and  $600 \text{ cm}^{-1}$ , at  $4\text{-cm}^{-1}$  spectral resolution with 64 scans. The background spectrum was obtained from a clean diamond-coated stick.

For comparison purposes, transmission FTIR spectra were collected with the same spectrometer in a diamond cell in the range between  $4000$  and  $600 \text{ cm}^{-1}$ , at  $4\text{-cm}^{-1}$  spectral resolution with 64 scans.

### Noninvasive FTIR reflection spectroscopy

Noninvasive FTIR reflection analyses were performed with a portable ALPHA-R spectrometer (Bruker Optics, Germany) equipped with a dedicated external reflection module, which allows contactless and noninvasive FTIR analysis with a room-temperature deuterated L-alanine-doped triglycine sulfate detector and a  $22^\circ/22^\circ$  optical layout. The laboratory model and the Renaissance painting were placed in front of the instrument at a distance of about 1 cm, and the integrated video camera provided the view of the sampling area of about 4 mm in diameter. Reflectance spectra were collected in the spectral range between  $7000$  and  $400 \text{ cm}^{-1}$ , with a spectral resolution of  $4 \text{ cm}^{-1}$ , and were expressed as pseudo-absorbance units [ $A' = \log(1/R)$ ]. The spectral acquisition was performed with 160 scans. The background was acquired from a gold mirror.

## Results and discussion

### Micro-transfection spectra of the colour layer

The micro-transfection method was firstly applied to the paint layer, where a highly infrared absorbing

material, magnesium hydroxide carbonate, was used as an extender of the CdS-based oil paint. The application of the micro-transfection method to the inorganic components (as obvious further components in a painting) was a mandatory test to evaluate how the spectral distortions due to the presence of strongly infrared absorbing materials could affect the spectral profile of the organic varnish to be identified.

Three spectra recorded in reflection mode from different areas of the same metal stick after the sampling from the paint model are reported in Fig. 3a. Comparison of the three spectra revealed that, in this specific case, the transfection regime is not completely achieved, and the three profiles differ considerably because of spectral distortions arising from the complex reflection process, which depends on the thickness of the sampled materials as well as their intrinsic optical properties. Variation in relative intensities as well as broadening and baseline tilt might be encountered as a result of Fresnel reflection [6], as well as scattering processes or the effect of the EFSWs arising from reflection from a metallic-like surface [12]. As an example, the detection of the  $\nu_1 + \nu_3$  combination band of  $\text{CO}_3^{2-}$  of the carbonate pigment at about  $2500 \text{ cm}^{-1}$  is a clear indication of a not negligible contribution of the volume reflection [20].

Among the different profiles recorded from the metallic stick, we selected the one showing greatest similarity with corresponding micro-transmission profile and directly compared it with both noninvasive reflection and transmission spectra (Fig. 3b).

The comparison of the spectrum acquired in micro-transfection mode with the spectrum acquired in transmission mode (Fig. 3b, black and blue lines) clearly highlights a broadening as well as a maxima shift ( $4\text{--}8 \text{ cm}^{-1}$ ) of the strong

$\nu_3 (\text{CO}_3^{2-})$  doublet, confirming the contribution of the volume reflection. In addition, the baseline profile with regard to the  $\nu_3$  band (Fig. 3a, b) indicates a not negligible contribution from the real part of the refractive index [6], suggesting that also surface reflection occurs. As observed in the noninvasive reflection spectrum in Fig. 3b, the  $\nu_3$  band appears strongly distorted by the anomalous dispersion of the refractive index [6], which also partially affects the micro-transfection spectrum.

Nevertheless, the distinctive vibrational pattern of hydrated magnesium carbonate is easily recognizable: the  $\nu_3$  mode resulting in a double band at  $1481 \text{ cm}^{-1}$  and  $1423 \text{ cm}^{-1}$  and a doublet at  $874 \text{ cm}^{-1}$  and  $855 \text{ cm}^{-1}$  ( $\nu_2 \text{CO}_3^{2-}$  bending modes). Finally, in good agreement with the transmission mode spectrum, the micro-transfection spectrum shows bands at  $3447 \text{ cm}^{-1}$ ,  $3512 \text{ cm}^{-1}$ , and  $3649 \text{ cm}^{-1}$  due to the O–H stretching modes of the hydrated carbonate [21, 22] as well as additional bands, at  $1666 \text{ cm}^{-1}$  and  $1598 \text{ cm}^{-1}$ , that could be assigned to the related OH bending.

Regarding the identification of the organic binder, the broadening and weak distortion of the  $\nu_3$  band ( $\text{CO}_3^{2-}$ ) partially covers the band assigned to the stretching of the carbonyl ester bond at about  $1740 \text{ cm}^{-1}$  appearing as a weak shoulder. Nevertheless, this weak signal in combination with the evident CH stretching modes at  $2900 \text{ cm}^{-1}$  allows the characterization of the lipidic medium.

It is worth noting that in the corresponding noninvasive reflection spectrum (Fig. 3b, red line) the characterization of the organic binder may be achieved only by exploration of the near-infrared region, showing the distinctive combination bands ( $\nu + \delta$ ) of methylenic C–H at  $4340 \text{ cm}^{-1}$  and  $4266 \text{ cm}^{-1}$  [23, 24], being the fingerprint

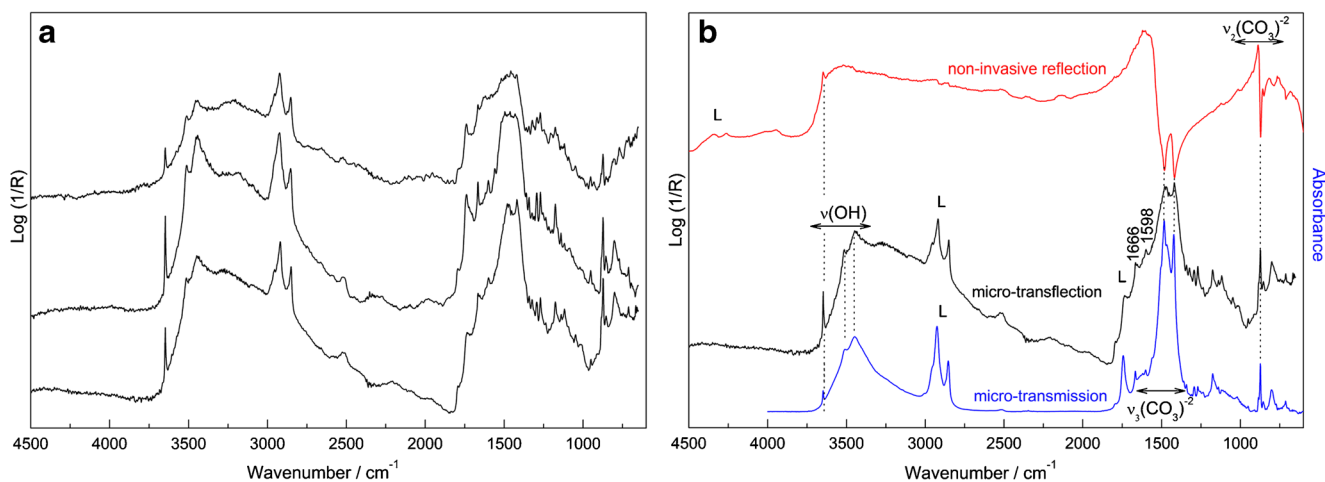


**Fig. 3** **a** Comparison of the different spectra recorded in transfection mode from the stick after one minimally invasive sampling. **b** Comparison of the spectral profiles recorded from the color layers with

the different acquisition modes: micro-transfection (black line), noninvasive reflection (red line) and micro-transmission (blue line). L bands of the lipidic binder

region predominantly dominated by the signal of the carbonate-based pigment.

### Micro-transflection spectra of varnish layers

The reliability of the micro-transflection spectra recorded on the selected varnishes after their sampling by the diamond-coated stick from the model was evaluated directly comparing the profiles with reference transmission data as reported in Table 1. The micro-transflection spectra are also compared in Fig. 4 with the corresponding noninvasive reflection profiles as propaedeutic study evaluating the applicability of the minimally invasive method as a tool supporting noninvasive reflection FTIR measurements.

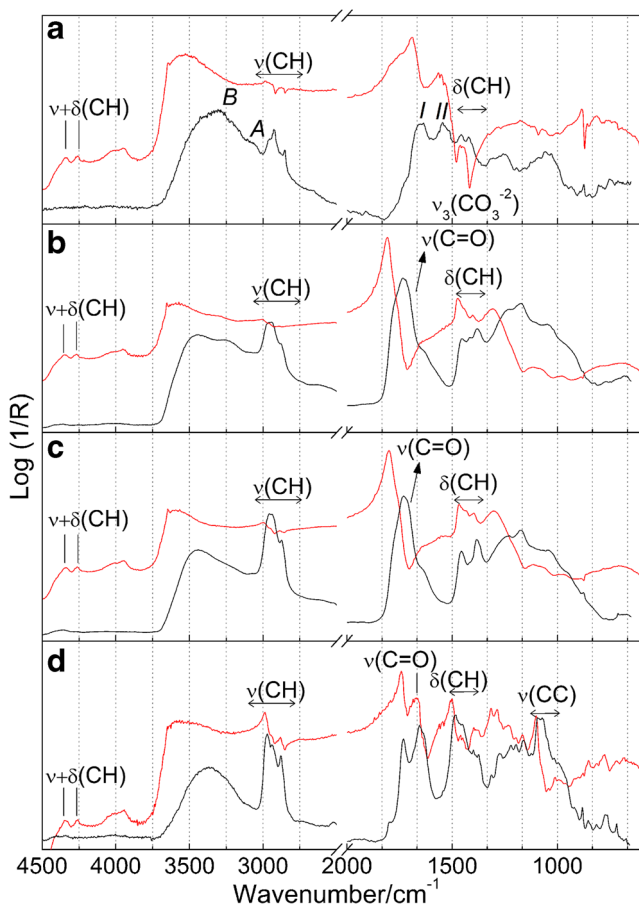
### Egg white varnish

Figure 4, panel a reports the micro-transflection spectrum of egg white varnish, applied over the oil colour layer, showing the characteristic FTIR bands of a proteinaceous compound. The strongest bands of egg white corresponding to amide I and amide II are clearly visible in the micro-transflection spectrum at  $1648\text{ cm}^{-1}$  and  $1546\text{ cm}^{-1}$ , shifted by only  $2\text{--}4\text{ cm}^{-1}$  with respect to the value obtained in transmission mode (Fig. 4, panel a, black line). An anomalous low amide I/amide II intensity ratio may be observed; as also discussed by Bassan et al. [8] this is the typical distortion of transflection spectra linked to the EFSW effect. Also the shift of the  $\delta\text{ CH}$  (at  $1452\text{ cm}^{-1}$ ) with respect to transmission mode is very

**Table 1** Experimental Fourier transform infrared wavenumbers of the varnishes studied

Varnish <sup>a</sup>	Micro- transflection ( $\text{cm}^{-1}$ )	Reflection ( $\text{cm}^{-1}$ )	Transmission ( $\text{cm}^{-1}$ )	Band assignment
Egg white	1059		1056	$\nu\text{ C-O}$
	1457		1452	$\delta\text{ CH}$
	1546	1560-1550	1548	Amide II
	1648	1660	1652	Amide I
	3060		3064	Amide B
	3300		3302	Amide A
Dammar	1048	1020	1049	$\delta_{\text{ring}}\text{ C-H}$
	1177	1150	1175	
	1230	1230/1220	1230	$\nu\text{ C-C}$
	1384	1397	1384	$\delta_{\text{AS}}\text{ CH}_2$
	1456	1476	1456	$\delta_{\text{S}}\text{ CH}_3$
	1732	1705-1800	1729	$\nu\text{ C=O}$
	2871	2862	2872	$\nu_{\text{S}}\text{ CH}_2$
	2954	2947	2958	$\nu_{\text{AS}}\text{ CH}_2$
	Mastic	1043	1018	1048
1176		1152	1174	
1237			1230	$\nu\text{ C-C}$
1382		1397	1385	$\delta_{\text{AS}}\text{ CH}_2$
1452, 1419		1476	1455	$\delta_{\text{S}}\text{ CH}_3$
1735		1705 – 1800	1729	$\nu\text{ C=O}$
2879		2862	2872	$\nu_{\text{S}}\text{ CH}_2$
2962		2947	2957	$\nu_{\text{AS}}\text{ CH}_2$
3451			3446	$\nu\text{ O-H}$
Laropal A 81	1066		1064	$\nu\text{ C-C}$
	1089	1080	1088	
	1447	1435	1446	$\delta_{\text{AS}}\text{ CH}_2$
	1480	1500-1480	1486	$\delta_{\text{S}}\text{ CH}_3$
	1650	1650	1651	Amide I
	1726	1730	1728	$\nu\text{ C=O}$
	2875	2870	2874	$\nu_{\text{S}}\text{ CH}_3$
	2934	2938	2932	$\nu_{\text{AS}}\text{ CH}_2$
	2967	2969	2967	$\nu_{\text{AS}}\text{ CH}_3$
	3360		3360	$\nu\text{ O-H}$

<sup>a</sup> Details on the exact composition of the studied varnishes are reported in “Materials and methods”



**Fig. 4** Noninvasive reflection (red line) and micro-transfection (black line) spectra of egg white (a), dammar (b), mastic (c), and Laropal A 81 (d) varnishes

small, ranging from 3 to 5  $\text{cm}^{-1}$ . In the higher-wavenumber range, the typical amide A and amide B bands at 3300  $\text{cm}^{-1}$  and 3060  $\text{cm}^{-1}$  are also visible [25, 26].

Diversely, the noninvasive identification of the proteinaceous finishing layer is complicated by the presence of the strong infrared absorbing hydrated magnesium carbonate present in the color layer (Fig. 4, panel a, red line). The infrared absorption properties of the protein-based layer favor the penetration of the infrared radiation, resulting in recording of mainly the underneath rather than the surface varnish. The strong  $\nu_3$  band of the carbonate anion totally hinders the CH bending mode and partially amide II bands, just permitting the visualization of the strongest amide I band at about 1660  $\text{cm}^{-1}$ .

#### Mastic and dammar varnishes

Mastic and dammar varnishes are discussed together since the infrared spectral profiles look very similar because the varnishes have an equivalent chemical composition based on terpenic compounds.

The direct comparison of the band maxima in the micro-transfection spectra of dammar and mastic with those observed in transmission mode (Table 1) highlights a rather good similarity. The strong band of the stretching vibrations of the carbonyl group (Fig. 4, panels b and c, black lines) is observed at approximately 1732  $\text{cm}^{-1}$  (dammar) and 1726  $\text{cm}^{-1}$  (mastic) for both acquisition modes and is in general agreement with the values reported for an aged terpenic resin in which oxidation processes occurred [27, 28]. The strong doublet of the methyl and methylene groups in the range from 1460 to 1390  $\text{cm}^{-1}$  for the micro-transfection spectrum perfectly matches the one visible in the transmission-mode spectrum of either dammar (at 1456  $\text{cm}^{-1}$  and 1384  $\text{cm}^{-1}$ ) or mastic (at 1452  $\text{cm}^{-1}$  and 1382  $\text{cm}^{-1}$ ) [29, 30]. The signal at approximately 1170  $\text{cm}^{-1}$  can be attributed to C–H bending vibration in the ring of dammar and mastic varnishes or to C–O stretching in the lipidic binder. The other intense bands of the stretching vibrations of C–H groups appearing at approximately 2954  $\text{cm}^{-1}$  and approximately 2871  $\text{cm}^{-1}$  in dammar and at 2962  $\text{cm}^{-1}$  and 2879  $\text{cm}^{-1}$  in mastic are slightly shifted by approximately 4–7  $\text{cm}^{-1}$  in comparison with the bands in the transmission spectra (Table 1).

The chemical similarity of dammar and mastic is also reflected in the total reflection infrared profile (Fig. 4, panels b and c, red lines). The optically flat surface generated by the organic layer favors the collection of surface reflection according to Fresnel's law [24]. Indeed, the reflection profile mainly follows the refractive index behavior, generating derivative-like bands corresponding to the absorption maxima. This clearly happens for the carbonyl stretching vibrations in the range from 1800 to 1700  $\text{cm}^{-1}$  (Fig. 4, panels b and c, red lines); weaker absorption bands are instead characterized by a broader derivative-like profile including also some portion of the volume reflection as the bending vibrations of the methylene and methyl groups at about 1400  $\text{cm}^{-1}$  and 1480  $\text{cm}^{-1}$  respectively. The greater penetration depth offered by the near-infrared range allows the identification of the lipidic medium (doublet at about 4340  $\text{cm}^{-1}$  and 4270  $\text{cm}^{-1}$  due to the  $\nu+\delta$  combination mode of CH [24]) from the paint layer. In the specific case of mastic, we may not exclude the possible contribution of the linseed oil added in the sample preparation.

#### Laropal A 81 varnish

In the micro-transfection spectrum of the synthetic varnish Laropal A 81 (Fig. 4, panel d, black line), a strong stretching vibration mode of the carbonyl group is present at 1726  $\text{cm}^{-1}$ . A significant band corresponding to stretching vibration of another carbonyl group of amide I is seen at 1650  $\text{cm}^{-1}$  and it is due to the urea content in Laropal A 81 [31]. A strong



absorption peak at  $1480\text{ cm}^{-1}$  and its shoulder at  $1447\text{ cm}^{-1}$  are assigned to the bending vibrations of the methyl and methylene groups respectively. In the fingerprint region, two strong signals of the synthetic varnish appear at  $1089\text{ cm}^{-1}$  and  $1066\text{ cm}^{-1}$ . Laropal A 81 has distinctive signals also in the region of asymmetric and symmetric stretching vibrations of C–H bonds; namely, at  $2875\text{ cm}^{-1}$ ,  $2934\text{ cm}^{-1}$ , and  $2967\text{ cm}^{-1}$ . These characteristic signals of Laropal A 81 obtained with the micro-transfection method are in good agreement with the absorbance bands in the transmission spectrum. The only observable modification is the shift of  $4\text{--}6\text{ cm}^{-1}$  (Table 1) of the bending vibration of methyl group.

The corresponding noninvasive reflection spectrum (Fig. 4, panel d, red line) shows all the aforementioned bands appearing as derivative and/or inverted signals. Also the peculiar CH stretching profile is similarly traced in reflection, highlighting the  $2870\text{ cm}^{-1}$  and  $2969\text{ cm}^{-1}$  stretching of Laropal A 81 as shoulders of the methylene CH of the lipid binder from the underneath layer.

#### FTIR monitoring of solvent cleaning on paint models

The good results in the identification of varnish layers with minimal sampling encouraged us to test the method in monitoring cleaning processes in combination and as a tool supporting noninvasive reflection FTIR spectroscopy. For the cleaning tests on the model painting, three different agents were used: acetone and two mixtures of acetone and ethanol in different volume ratios: 3:7 and 4:6 respectively. The cleaning agents were applied on the uppermost varnish layers (dammar, mastic, Laropal A 81). For the locations of the cleaning areas, see Fig. 1c. The cleaning of mastic applied over egg white is presented here.

Micro samples were collected with the diamond-coated stick after the cleaning treatments. For each cleaning test, one sampling was performed. Under the FTIR microscope it was possible to probe different areas (up to five) at the top of the stick containing the sample. The most representative spectra for each cleaned sector are reported in Fig. 5.

#### Monitoring of the cleaning of a mastic-varnished sector applied over egg white varnish

Firstly the laboratory model was monitored by noninvasive reflection FTIR spectroscopy: the spectra of the cleaned areas compared with the spectrum of the mastic-varnished model before the cleaning are shown in Fig. 5, panel a. All the noninvasive reflection spectra of the cleaned sectors are affected by the high infrared absorbing layer underneath (paint layer) as the varnish layer has been considerably thinned during the cleaning process. The cleaning tests using 3:7 acetone and ethanol and 4:6 acetone and ethanol gave similar spectral profiles (Fig. 5, panel a, blue and green lines), highlighting partial

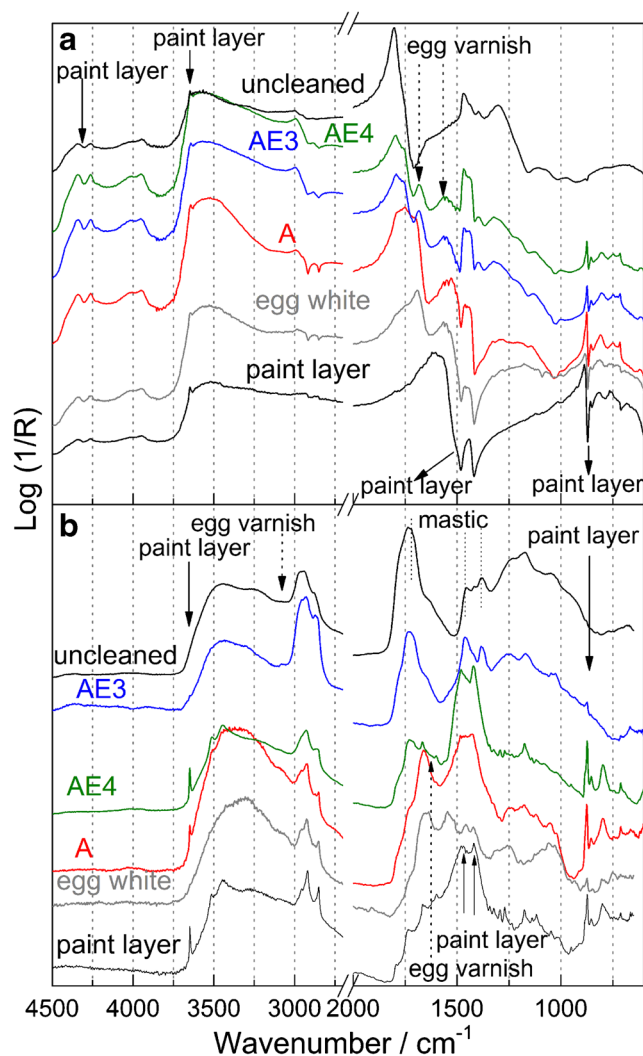


**Fig. 5** Spectra recorded in noninvasive reflection mode (a) and micro-transfection mode (b) of the uncleaned mastic varnished layer, the egg white layer, the paint layer, and the different cleaning areas. A acetone, AE3 3:7 acetone and ethanol, AE4 4:6 acetone and ethanol

removal of the external mastic varnish and the appearance of the protein signals (amide I and amide II marked with dotted arrows in Fig. 5, panel a) of the inner layer of varnish. The higher degree of removal by the acetone cleaning is highlighted by the stronger contribution in the spectral profile of the bands relative to the paint layer (Fig. 5, panel a, marked with solid arrows). The spectral region including the carbonyl band of the natural resin and the amide I band of the inner protein-based varnish ( $1800\text{--}1500\text{ cm}^{-1}$ ) is characterized by a broadened derivative-like feature (comprising the two contributions) and whose interpretation is not straightforward.

Micro-transfection spectra of the cleaning areas on the mastic-varnished paint are reported in Fig. 5, panel b. In agreement with the noninvasive investigation, the cleaning methods using 3:7 acetone and ethanol and 4:6 acetone and ethanol partially removed the surface varnish layer, revealing the infrared bands of the underneath egg varnish (dotted arrow in



Fig. 5, panel b) and the paint layer (solid arrows in Fig. 5, panel b). According to the micro-transfection data, the extent of the cleanings by 3:7 acetone and ethanol and 4:6 acetone and ethanol are quite different, highlighting a greater removal degree for 4:6 acetone and ethanol, whereas with noninvasive reflection the effect of the two cleaning methods was equivalent. This may be explained by consideration of the different spatial resolution in the sampling of the two FTIR methods; the noninvasive reflection technique allows a larger area (about 12 mm<sup>2</sup>) to be investigated.

### Monitoring of the cleaning of a Renaissance painting

The capabilities of monitoring a cleaning procedure through a combined approach based on micro-transfection FTIR and non-invasive reflection FTIR techniques were finally studied for a Renaissance painting: *Presentation in the Temple* by Vittore Carpaccio. The artwork was subjected to a wax-resin lining during the conservation–restoration procedure which occurred between 1958 and 1961, although at least one restoration intervention occurred before that time. Wax-resin lining treatment was a common practice in the past and was extremely popular throughout Europe, especially during the twentieth century, but now resulting, along with the surface dirt deposits and darkened nonoriginal varnish layers, in a global darkening of the painting. The aforementioned and additional reasons (inadequate retouchings, overpaintings, etc.) required a cleaning treatment aimed at the removal of the nonoriginal materials that distorted the visual appearance of the painting.

A noninvasive reflection spectrum representative of the uncleaned surface is reported in Fig. 6, panel a. The combined presence of a sharp doublet in the near-infrared range at about 4300 cm<sup>-1</sup>, strong and sharp CH stretching at about

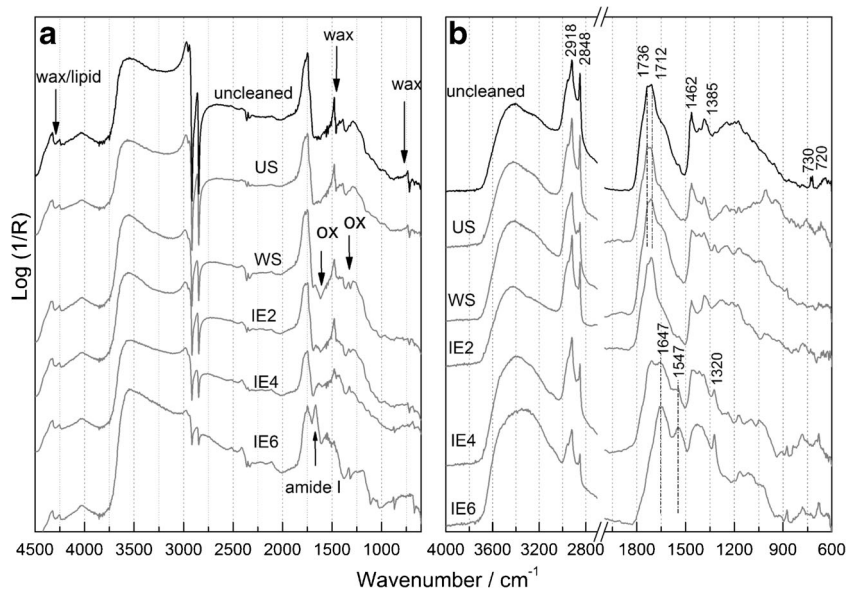
3000 cm<sup>-1</sup>, derivative-like CH bending modes at 1470 cm<sup>-1</sup> and 1460 cm<sup>-1</sup>, and CH rocking (at 730 cm<sup>-1</sup> and 715 cm<sup>-1</sup>) confirmed the use of a long-chain hydrocarbon compound like wax along with the presence of a lipidic compound probably used as a binding medium. The noninvasive reflection profile of the uncleaned area also shows a broad carbonyl stretching (in the range from 1800 to 1700 cm<sup>-1</sup>; Fig. 6, panel a), thus suggesting the presence of an additional organic compound, which, however, was not straightforwardly identified.

The nature of this additional component was revealed by the micro-transfection method performed on the uncleaned area. The corresponding spectrum (Fig. 6, panel b, uncleaned area) showed the bands relative to wax (sharp CH stretching at 3000 cm<sup>-1</sup>, carbonyl stretching at 1740 cm<sup>-1</sup>, and the CH rocking doublet at 730 cm<sup>-1</sup> and 720 cm<sup>-1</sup>) also identified by the noninvasive method. Furthermore, the more conventional spectral profile obtained by the micro-transfection method allowed the detection of additional bands (the carbonyl stretching at 1710 cm<sup>-1</sup> and the CH bending modes at 1470 cm<sup>-1</sup> and 1380 cm<sup>-1</sup>), revealing the use of a terpenic varnish [29, 30].

Once the nature of the surface organic materials had been identified, the restorers selected the most appropriate set of cleaning methods to be monitored by the proposed analytical approach. The spectral profiles recorded in the cleaned areas by the two FTIR techniques are compared with the uncleaned profiles in Fig. 6.

The wider spectral window (6000–400 cm<sup>-1</sup>) available in the noninvasive reflection spectra, including also the near-infrared range, allows different depths of the painting to be probed. In the near-infrared range (thus exploring the inner layers) there is no effect on the CH combination bands of wax (at 4300 cm<sup>-1</sup>) after the different cleaning methods

**Fig. 6** Noninvasive reflection Fourier transform infrared spectra (a) and micro-transfection Fourier transform infrared spectra (b) of the uncleaned area and areas cleaned with different solvents. IE2 20:80 isooctane and ethanol, IE4 40:60 isooctane and ethanol, IE6 60:40 isooctane and ethanol, ox oxalate, US artificial saliva, WS white spirit



mainly affecting the surface layers. Conversely, in the low-wavenumber range the thinning of the surface wax is monitored by the decrease of the CH rocking band at  $730\text{--}720\text{ cm}^{-1}$  (Fig. 6, panel a). The results indicate that only the cleanings with 40:60 isooctane and ethanol and 60:40 isooctane and ethanol resulted in the removal of the wax present on the surface (Fig. 6, panel a, wax). The origin of this surface wax could be from a portion of wax migrating toward the surface owing to the lining treatment. However, an undocumented past restoration intervention including the application of a surface varnish containing a long-chain hydrocarbon like a wax cannot be excluded.

The cleaning performed with the artificial saliva showed an infrared spectral profile very similar to the uncleaned one, suggesting that no removal occurred (Fig. 6, panel a, US). The use of the white spirit and 20:80 isooctane and ethanol allowed partial removal of the surface wax (Fig. 6, panel a, WS and IE2), thus permitting the discrimination of the bands relative to the terpenic natural varnish. They are mainly in the same range as those of wax (the carbonyl in the  $1800\text{--}1700\text{ cm}^{-1}$  range and the CH bending mode at about  $1480\text{ cm}^{-1}$ ) but are characterized by spectral shapes broadened by the volume reflection and thus distinguishable by the derivative-like profile of wax. The decrease of the varnish layer was accompanied by the appearance of the oxalate bands (at  $1320\text{ cm}^{-1}$  and  $1600\text{ cm}^{-1}$  [32]), indicating that under the varnish there was an oxalate patina; this situation is often encountered when the removal of varnishes on ancient paintings is investigated [32, 33]. The spectral profile recorded in the sector cleaned with 40:60 isooctane and ethanol did not show the signals of wax, which has been removed; it is characterized by a reduced broadening of carbonyl stretching (here related to the terpenic resin on the basis of micro-transflection spectra) as well as the oxalate signals (Fig. 6, panel a, IE4). Only with the cleaning with 60:40 isooctane and ethanol was the terpenic varnish also removed, reaching the painting layer composed of lead white (combination band at  $2400\text{ cm}^{-1}$  [20]) and possibly a lipidic binder (CH combination bands at  $4300\text{ cm}^{-1}$ , carbonyl stretching at  $1740\text{ cm}^{-1}$  [24]) (Fig. 6, panel a, IE6). In addition, a band at about  $1670\text{ cm}^{-1}$  appeared in the noninvasive infrared profile and whose assignment was not certain. This could be an indication of the possible presence of a protein-based compound (amide I band); nevertheless, the presence of the carbonate anion of lead white strongly influences this spectral range, making any assignment very difficult.

To better interpret the infrared spectrum, the corresponding micro-transflection profile through the minimally invasive method was required. The resulting spectrum (Fig. 6, panel b, IE6) revealed without any doubt the presence of a proteinaceous compound showing both the amide I band and the amide II band (at  $1650\text{ cm}^{-1}$  and  $1550\text{ cm}^{-1}$  respectively) as well as the amide B band along with the antisymmetric stretching of the carbonate anion in lead white at  $1410\text{ cm}^{-1}$

and oxalate signals at  $1322\text{ cm}^{-1}$ . The protein signals may be present for two reasons: the application of egg tempera in the paint layer and/or the use of another proteinaceous varnish layer beneath the uppermost layers of varnishes.

The micro-transflection method performed on the sector cleaned with 40:60 isooctane and ethanol indicated the presence of a proteinaceous material undetectable by the noninvasive method because of the higher spectral distortions due to the inorganic counterpart (Fig. 6, IE4).

## Conclusion

Micro-transflection FTIR spectroscopy on a diamond-coated metallic stick has been proved to be valuable method for the molecular identification of varnishes on the surface of easel paintings.

The use of a metallic substrate under a micro-FTIR spectrometer allows one to work in a micro-transflection regime, the spectra acquired being in very good agreement with transmission data and thus providing an easy interpretation.

The high sensitivity provided by the transflection acquisition mode allows minimally invasive sampling that is barely visible to the naked eye and thus preferable to a traditional microsampling for transmission micro-FTIR spectroscopy on diamond cell. Finally, since no sample manipulation is necessary, no information on the surface compound is lost.

These positive results may be extended only partially to the inorganic painting materials. Some tests on the magnesium carbonate hydrate revealed spectral distortions due to the difficulty of achieving sample deposition optically transparent to the infrared radiation. The sampling of highly infrared absorbing materials may more easily result in an optically dense layer favoring the surface and volume reflection—with the associated spectral distortion—with respect to the transmission of the infrared light.

For the identification of weakly infrared absorbing thin layers of organic varnish applied over highly infrared absorbing inorganic materials (i.e., the model with egg white varnish applied over the paint layer), the micro-transflection technique works better than the noninvasive reflection method, which, instead, mostly reveals the material beneath.

The present study also demonstrated the value of the micro-transflection approach when applied in combination with noninvasive reflection FTIR spectroscopy in monitoring the effect of solvent cleaning.

If the latter serves for the global survey of the painting surface by a representative number of measurements (after as well as before the cleaning), the first aids in the molecular identification, helping in the interpretation of often complicated spectral patterns appearing in the noninvasive reflection mode.

**Acknowledgements** This work was performed with the support of the European Commission through the project Iperion CH, H2020-INFRAIA-2014-2015 (grant no. 654028). The authors thank Maša Kavčič and Barbka Gosar Hirci, Department of Easel Painting, Restoration Center, Institute for the Protection of the Cultural Heritage of Slovenia, for a fruitful discussion and help with the cleaning tests on the case study painting *Presentation in the Temple* by Vittore Carpaccio.

#### Compliance with ethical standards

**Conflict of interest** The authors declare that they have no conflict of interest.

#### References

- Rosenzweig B, Carretti E, Picollo M, Baglioni P, Dei L. Use of mid-infrared fiber-optic reflectance spectroscopy (FORS) to evaluate efficacy of nanostructured systems in wall painting conservation. *Appl Phys A Mater.* 2006;83:669–73.
- Carretti E, Rosi F, Miliani C, Dei L. Monitoring of pictorial surfaces by mid-FTIR reflectance spectroscopy: evaluation of the performance of innovative colloidal cleaning agents. *Spectrosc Lett.* 2005;38:459–65.
- Kahrim K, Daveri A, Rocchi P, de Cesare G, Cartechini L, Miliani C, et al. The application of in situ mid-FTIR fibre-optic reflectance spectroscopy and GC–MS analysis to monitor and evaluate painting cleaning. *Spectrochim Acta A.* 2009;74(5):1182–8.
- Ormsby B, Kampasakali E, Miliani C, Learner T. An FTIR-based exploration of the effects of wet cleaning treatments on artists' acrylic emulsion paint films. *e-PS.* 2009;6:186–95.
- Tavzes Č, Šilc F, Kladnik A, Fackler K, Messner K, Pohleven F, et al. Enzymatic degradation of mould stains on paper analysed by colorimetry and DRIFT-IR spectroscopy. *Int Biodeterior Biodegrad.* 2009;63:873–9.
- Griffith R, de Haseth A. *Transfection.* In: Fourier transform infrared spectrometry. Totowa: Wiley; 2007. p. 297–300.
- Koçak A, Lucania JP, Berets SL. Some advances in Fourier transform infrared transfection analysis and potential applications in forensic chemistry. *Appl Spectrosc.* 2009;63:507–11.
- Bassan P, Lee J, Sachdeva A, Pissardini J, Dorling KM, Fletcher JS, et al. The inherent problem of transfection-mode infrared spectroscopic microscopy and the ramifications for biomedical single point and imaging applications. *Analyst.* 2013;138:144–57.
- Perez-Guaita D, Heraud P, Marzec M, de la Guardia M, Kiupel M, Wood BR. Comparison of transfection and transmission FTIR imaging measurements performed on differentially fixed tissue sections. *Analyst.* 2015;140:2376–82.
- Wehbe K, Filik J, Frogley MD, Cinque G. The effect of optical substrates on micro-FTIR analysis of single mammalian cells. *Anal Bioanal Chem.* 2013;405:1311–24.
- Koçaka A, De Cotiis LM, Hoffman DB. Comparative study of ATR and transfection IR spectroscopic techniques for the analysis of hallucinogenic mushrooms. *Forensic Sci Int.* 2010;195:36–41.
- Filik J, Frogley MD, Pijanka JK, Wehbe K, Cinque G. Electric field standing wave artefacts in FTIR micro-spectroscopy of biological materials. *Analyst.* 2012;137:853–61.
- Boyatzis SC, Douvas AM, Argyropoulos V, Siatou A, Vlachopoulou M. Characterization of a water-dispersible metal protective coating with Fourier transform infrared spectroscopy, modulated differential scanning calorimetry, and ellipsometry. *Appl Spectrosc.* 2012;66(5):580–90.
- Argyropoulos V, Boyatzis S, Giannoulaki M, Polikreti K. The role of standards in conservation methods for metals in cultural heritage. In: Dillmann P, Watkinson D, Angelini E, Adriaens A, editors. *Corrosion and conservation of cultural heritage metallic artefacts*, European Federation of Corrosion (EFC) Series. Woodhead Publishing Limited; 2013. p. 478–517.
- Ropret P, Legan L, Rosi F, Miliani C. A novel approach for micro FTIR reflection absorption analysis of artworks' surface. In: Rogerio-Candellera M, Lazzari M, Cano E, editors. *Proceedings of the international congress science and technology for the conservation of cultural heritage*. Santiago de Compostela Spain: CRC Press; 2012. p. 189–92.
- Feller RL, Stolow N, Jones EH. *On picture varnishes and their solvents.* London: The Press of Case Western Reserve University; 1971.
- Wehlte K. *The materials and techniques of painting.* New York: Van Nostrand Reinhold; 1975.
- René de la Rie E, Lomax SQ, Palmer M, Maines CA. In: ICOM committee for conservation, ICOM-CC: 13th triennial meeting, Rio de Janeiro, 22-27 September 2002. London: James & James; 2002. p. 881–887.
- Stoner JH, Rushfield R. *The conservation of easel paintings.* London: Routledge; 2012.
- Miliani C, Rosi F, Daveri A, Brunetti BG. Reflection infrared spectroscopy for the non-invasive in situ study of artists' pigments. *Appl Phys A.* 2012;106:295–307.
- Farmer VC. *The infrared spectra of minerals.* London: Mineralogical Society; 1974.
- Learner TJS. *Analysis of modern paints.* Los Angeles: Getty Publications; 2004.
- Vagnini M, Miliani C, Cartechini L, Rocchi P, Brunetti BG, Sgamellotti A. FT-NIR spectroscopy for non-invasive identification of natural polymers and resins in easel paintings. *Anal Bioanal Chem.* 2009;395:2107–18.
- Rosi F, Daveri A, Moretti P, Brunetti BG, Miliani C. Interpretation of mid and near-infrared reflection properties of synthetic polymer paints for the non-invasive assessment of binding media in twentieth-century pictorial artworks. *Microchem J.* 2016;124:898–908.
- Barth A, Zscherp C. What vibrations tell us about proteins. *Q Rev Biophys.* 2002;35:369–430.
- Rozenberg M, Shoham G. FTIR spectra of solid poly-L-lysine in the stretching NH mode range. *Biophys Chem.* 2007;125:166–71.
- Azémar C, Vieillescazes C, Ménager M. Effect of photodegradation on the identification of natural varnishes by FT-IR spectroscopy. *Microchem J.* 2014;112:137–49.
- Dietemann P, Higgitt C, Kälin M, Edelmann MJ, Knochenmuss R, Zenobi R. Aging and yellowing of triterpenoid resin varnishes – influence of aging conditions and resin composition. *J Cult Herit.* 2009;10:30–40.
- Theodorakopoulos C, Zafirooulos V, Boon JJ, Boyatzis SC. Spectroscopic investigations on the depth-dependent degradation gradients of aged triterpenoid varnishes. *Appl Spectrosc.* 2007;61:1045–50.
- Nevin A, Comelli D, Osticioli I, Toniolo L, Valentini G, Cubeddu R. Assessment of the ageing of triterpenoid paint varnishes using fluorescence, Raman and FTIR spectroscopy. *Anal Bioanal Chem.* 2009;95:2139–49.
- Zhang YF, Zeng XR. One-pot synthesis and structural characterization of urea-isobutyraldehyde-formaldehyde resin. *J Cent South Univ Technol.* 2009;16:80–4.
- Monico L, Rosi F, Miliani C, Daveri A, Brunetti BG. Non-invasive identification of metal-oxalate complexes on polychrome artwork surfaces by reflection mid-infrared spectroscopy. *Spectrochim Acta A.* 2013;116:270–80.
- Van der Snickt G, Miliani C, Janssens K, Brunetti BG, Romani A, Rosi F, et al. Material analyses of 'Christ with singing and music-making Angels', a late 15th-C panel painting attributed to Hans Memling and assistants: part I. Non-invasive in situ investigations. *J Anal At Spectrom.* 2011;26:2216–29.